Int. J. Multiphase Flow Vol. 15, No. 5, pp. 831–841, 1989
Printed in Great Britain.

0301-9322/89 $3.00 + 0.00

UNSTABLE FLOW OF A SOLID–LIQUID MIXTURE IN A HORIZONTAL PIPE

H. TAKAHASHI, T. MASUYAMA and K. NODA
Department of Resources Engineering, Tohoku University, Sendai 980, Japan

(*Received* 14 *December* 1988; *in revised form* 31 *May* 1989)

Abstract—Solid–liquid mixture flow at low velocities was investigated experimentally and theoretically. A typical flow characteristic is the formation of dunes in the pipe, causing a pressure fluctuation through their movement. The velocity of the dunes increased as the mean velocity of the mixture increased. The pressure fluctuation increased slightly as the solid concentration increased up to 10%. The power spectral density function (PSD) of the pressure fluctuation was also obtained to investigate the periodicity. Results indicated the existence of a dominant frequency. This dominant frequency was related to the movement of the dunes and it increased with an increase in the velocity of the dunes. The pressure fluctuation was numerically simulated, based on an assumed PSD. The simulated results of the pressure fluctuation were in good agreement with the experiments.

Key Words: solid–liquid mixture, pressure fluctuation, flow behavior of dunes, power spectral density function, dominant frequency

1. INTRODUCTION

Solid–liquid mixture flows are commonly encountered in several fields of industry, such as chemical processing plants, the mining of coal and other ores, and dredging. In many previous studies and operations, fine particles have been used. In such cases, the particles are uniformly dispersed in a carrier fluid at high velocities, and the flow is treated as a single-phase flow. On the other hand, the hydraulic transport of coarse particles has recently received considerable attention because of the reduction in crushing and dewatering costs (Miscoe & Faddick 1980; Shook *et al.* 1981; Duckworth *et al.* 1983). Flows containing coarse particles cannot be treated as single-phase flows because the particles are affected by gravitational force and therefore move in the lower part of the pipe (Wilson *et al.* 1972; Televantos *et al.* 1979; Noda *et al.* 1980). Such flows are often analyzed using a two-layer model.

In designing a hydraulic transport system for coarse particles, it is very important to determine the transport velocity and to estimate the pressure loss. For economic reasons, the transport velocity is usually set close to the critical velocity which is associated with minimum pressure loss. Therefore, much work has been done on the critical velocity and pressure loss. The critical velocity, however, is close to the limit deposit velocity. When the transport velocity is set near the critical velocity there is a risk of pipe blockage, caused by a small decrease in the transport velocity. Therefore, the behavior of the particles and the pressure loss of the flow at low velocities (e.g. of the order of the limit deposit velocity, the critical velocity) have to be fully investigated in order to prevent pipe blockages and also to transport particles securely and reliably.

Toda *et al.* (1977, 1978, 1980) measured the pressure loss of solid–liquid flow at low velocities and found that the pressure loss of the flow with a deposit bed was different from that with a moving bed. They also studied the limit deposit velocity and found that it depended on the particle–liquid density ratio, particle diameter, pipe diameter and solid concentration.

Tsuji *et al.* (1982, 1984) examined the pressure fluctuation in the pneumatic transport of solid particles in pipes. They measured the pressure fluctuation by using a pressure transducer, and obtained the auto-correlation function, the cross-correlation function and the power spectral density function (PSD). In their paper, it was shown that the pressure fluctuation was very small in suspending flows, and that it increased as the mean velocity decreased.

Noda *et al.* (1980, 1984) investigated the limit deposit velocity and pressure loss of the flow with a deposit bed experimentally and theoretically, based on a force balance model. In their experiment,

the limit deposit velocity had a maximum at a certain solid concentration, and the effects of factors such as the length and height of saltating particles were determined.

Wilson *et al.* (1972) studied the limit deposit velocity via a slip model, and proposed an equation to calculate the pressure loss at the slip point.

Condolios & Chapus (1963) concluded that the equation proposed by Durand (1953) could be used to calculate the pressure loss of the flow with a deposit bed if the hydraulic mean diameter was used instead of the pipe diameter.

Carstens (1969) proposed a theoretical model to estimate the pressure loss of the flow with a deposit bed. This model, however, included many suppositions. For instance, he assumed that the particle velocity was equal to that of the fluid, and that the friction coefficient for the surface of the bed was equal to that for the pipe wall. Therefore, this model is not applicable to coarse particle cases.

Shook & Daniel (1965) proposed a two-dimensional model to predict the pressure loss of the flow with a deposit bed.

As stated above, most previous studies were on the pressure loss or limit deposit velocity, and little work has been done on the unstable behavior of particles at low velocities. The tendency of the flow at low velocities is to form dunes in the pipe, and a pressure fluctuation results due to the movement of the dunes. As mentioned above, little work has been done on the dunes formed in a pipe at low velocities. Therefore, the objectives of the present study are to investigate the behavior of the dunes and pressure fluctuation in a pipe experimentally, and also to numerically simulate the pressure fluctuation by assuming its PSD.

2. THEORETICAL STUDIES ON THE MAXIMUM AMPLITUDE OF THE PRESSURE FLUCTUATION

Figure 1 shows a schematic diagram of the dunes formed in the pipe. In this figure: V_G is the dune velocity; H_b is the height of the particle layer formed at the pipe bottom; H is the height of the dunes; V_1 and V_2 are velocities of the fluid at the moving cross sections 1 and 2, respectively; A_0 is the total pipe area; and A_b and $A_b + A_s$ are the cross-sectional areas of the particle layer at the moving cross sections 1 and 2, respectively.

Let us start with the continuity equation for the fluid and solid particles. It is assumed for simplicity that the time-averaged cross-sectional area of the dunes is $A_b + A_s/2$. By assuming no slip between the fluid and solid particles in the particle layer, these equations are given by:

fluid,

$$V_1 A_1 = V_2 A_2 = V_m A_0 (1 - C_v) - \left(A_b + \frac{A_s}{2}\right) \epsilon V_G; \qquad [1]$$

and

particles,

$$V_m A_0 C_v = V_G \left(A_b + \frac{A_s}{2}\right)(1 - \epsilon); \qquad [2]$$

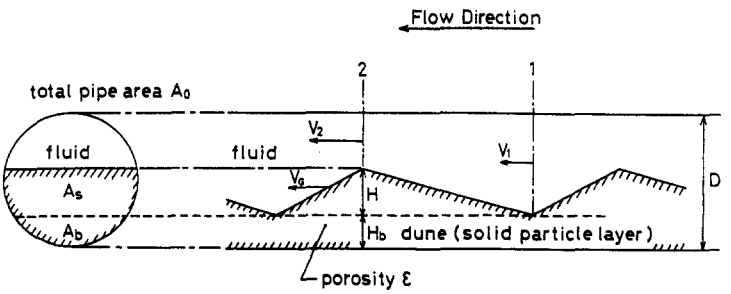

Figure 1. Schematic diagram of the dunes formed in the pipe.

where: V_m is the mean velocity of the mixture in the pipe (superficial velocity of the mixture with homogeneous flow assumption); V_G is the dune velocity; ϵ is the porosity of the particle layer; C_v is the delivered solid concentration; and A_1 and A_2 are the cross-sectional areas of fluid flow above the particle layer at the moving cross sections 1 and 2, respectively.

Here, we define the *in-situ* solid concentration C_T as

$$C_T = \frac{\text{Effective cross-sectional area of particles (time-averaged)}}{\text{Total pipe area}} = \frac{\left(A_b + \frac{A_s}{2}\right)(1-\epsilon)}{A_0}. \quad [3]$$

Using [3], the continuity equations for the fluid and particles, [1] and [2], are rewritten, respectively, as

$$V_1 A_1 = V_2 A_2 = V_m A_0 \left[1 - \frac{C_v}{(1-\epsilon)}\right] \quad [4]$$

and

$$\zeta \equiv \frac{V_G}{V_m} = \frac{C_v}{C_T}. \quad [5]$$

By considering that A_1 and A_2 are given, respectively, by

$$\frac{A_1}{A_0} = \frac{(A_0 - A_b)}{A_0} = 1 - \overline{A_b} \quad [6]$$

and

$$\frac{A_2}{A_0} = \frac{[A_0 - (A_b + A_s)]}{A_0} = 1 + \overline{A_b} - \frac{2C_v}{\zeta\,(1-\epsilon)}, \quad [7]$$

where

$$\overline{A_b} = \frac{A_b}{A_0}, \quad [8]$$

the fluid velocities V_1 and V_2 are expressed, in terms of V_m, by

$$V_1 = \frac{1 - \frac{C_v}{(1-\epsilon)}}{1 - \overline{A_b}} V_m \quad [9]$$

and

$$V_2 = \frac{1 - \frac{C_v}{(1-\epsilon)}}{1 + \overline{A_b} - \frac{2C_v}{\zeta(1-\epsilon)}} V_m. \quad [10]$$

In this paper, the maximum amplitude of the pressure fluctuation due to the movement of the dunes is assumed to be equal to the difference in pressure at cross sections 1 and 2. As will be described later, it was confirmed from experiments on the pressure fluctuation that most of the detected frequency components of the pressure fluctuation fall below 1.0 Hz. The fluid flow above the dunes, therefore, can be considered to be a quasi-steady flow. Using Bernoulli's theorem, the maximum amplitude of the pressure fluctuation dP is expressed by

$$dP \equiv P_1 - P_2 = \frac{\rho_w}{2}(V_2^2 - V_1^2), \quad [11]$$

where ρ_w is the density of the fluid. By substituting [9] and [10] into [11], we finally obtain the following expression for dP:

$$dP = \frac{\rho_w}{2} V_m^2 \left(1 - \frac{C_v}{1-\epsilon}\right)^2 \left\{\left[\frac{1}{1 + \overline{A_b} - \frac{2C_v}{\zeta(1-\epsilon)}}\right]^2 - \left(\frac{1}{1-\overline{A_b}}\right)^2\right\}. \quad [12]$$

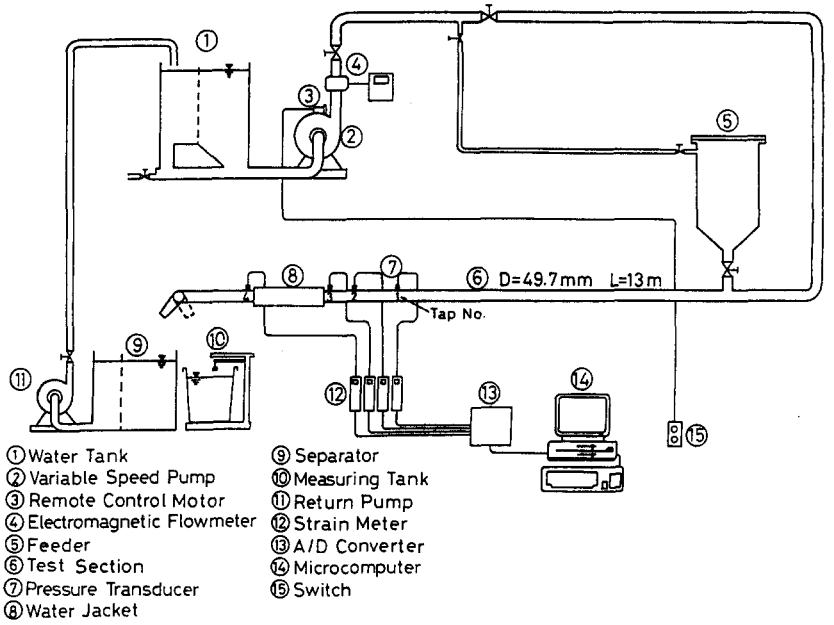

Figure 2. Schematic diagram of the experimental apparatus.

3. EXPERIMENTAL STUDIES

3.1. Experimental Apparatus and Procedure

Figure 2 shows a schematic diagram of the experimental apparatus used in this study. It consists of a water tank, a pump with a variable-speed drive, an electromagnetic flowmeter, a horizontal test section, pressure transducers, a water jacket and a measuring tank. The test section is a 13 m long transparent acrylic pipe with 49.7 mm i.d. to allow visual observation of the particle behavior by a videocamera. The test section is covered with a quadrilateral acrylic water jacket in order to eliminate the refraction of light by the curvature of the circular transparent pipe.

The pressure fluctuation was measured by strain gauge type pressure transducers at four different locations in the flow direction. These pressure transducers, with a dynamic pressure range of 50 kPa, were calibrated prior to the measurements. The pressure signals were transmitted through a strain meter and an A/D converter to a microcomputer, and the converted data were stored on magnetic disks in a digital manner. The sampling interval Δt was chosen as 10 ms so as to satisfy the sampling theorem (Bendat & Piersol 1966), given by

$$\Delta t \leqslant \frac{1}{2 \cdot f_c}, \qquad [13]$$

where f_c is the maximum effective frequency of the fluctuating signal. The total sampling time was 61.44 s. The upper cutoff frequency of a low-pass filter was set at 10 Hz, which was sufficient to detect the pressure fluctuation caused by the concentration fluctuation (Keska 1984) and to assure reliable of the measurements.

As mentioned earlier, one of the typical characteristics of a solid–liquid mixture flow in a horizontal pipe at low velocities is to form dunes. These dunes move slowly in the flow direction, and the period of the pressure fluctuation due to the movement of the dunes is considerably large, i.e. 3–4 s, as will be described. So, the total sampling time of 61.44 s is large enough to obtain reliable results for the pressure fluctuation.

The shape and velocity of the dunes were measured by a high-speed videocamera (NAC HSV-400) with a maximum of 400 fps. To assure easy visual observation of the particle behavior, a small fraction ($\sim$3%) of the particles (crushed rock) were carefully painted with white coloring.

The particle sizes covered in this study were 2.18 and 3.06 mm; other properties of the particles are listed in table 1.

Table 1. Particle properties

Material	Particle diameter, d_s (mm)	Specific gravity, S	Terminal velocity, V_{ss} (m/s)	Particle Reynolds number, Re_s	Drag coefficient, C_D
Crushed rock	2.18	2.74	0.16	443	1.92
	3.06		0.19	749	1.88

3.2. Experimental Results

3.2.1. Velocity of the dunes

Figure 3 shows the relationship between the ratio ζ of the dune velocity V_G to the mean velocity V_m and the solid concentration C_v with the particle diameter as a parameter. Here, V_m and V_G were measured by the electromagnetic flowmeter and high-speed videocamera, respectively. As shown in the figure, the value of ζ remains almost constant (about 0.54) regardless of the solid concentration. This means that the velocity of the dunes increases as the mean velocity V_m increases.

3.2.2. Particle layer thickness

Figure 4 shows the relationship between the dimensionless minimum particle layer thickness $\overline{H_b}$ and the solid concentrations C_v with the particle diameter as a parameter. At concentrations $<4\%$, the results show nearly zero $\overline{H_b}$. On the other hand, at concentrations $>4\%$, the value of $\overline{H_b}$ increased with increasing solid concentration. The solid line in figure 4 shows the following empirical equation, obtained by least squares fitting:

$$\overline{H_b} = 3.1\, C_v - 0.13 \qquad (C_v : \%). \tag{14}$$

As typically shown in figure 4, $\overline{H_b}$ is not affected by the particle size. Newitt *et al.* (1955) measured the pressure loss of the flow with a moving bed, and proposed the following equation for the pressure loss coefficient ϕ:

$$\phi = \frac{66(S-1)gD}{V_m^2}, \tag{15}$$

where ϕ is defined as in [16] below, S is the specific gravity of the particles and g is the gravitational acceleration;

$$\phi = \frac{(i - i_w)}{(i_w C_v)}, \tag{16}$$

i and i_w are the hydraulic gradients of the solid–liquid mixture flow and clear water, respectively.

This equation indicates no effect of particle size on the pressure loss of the flow with a moving bed. By considering this and the results shown in figures 3 and 4, it may be concluded that the behavior of particles in the pipe is independent of particle size for the flow with a moving bed.

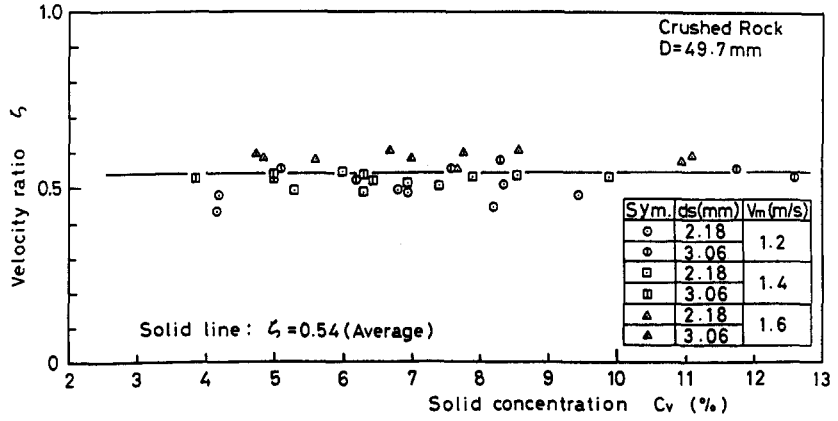

Figure 3. Velocity ratio of the dunes to the mean velocity.

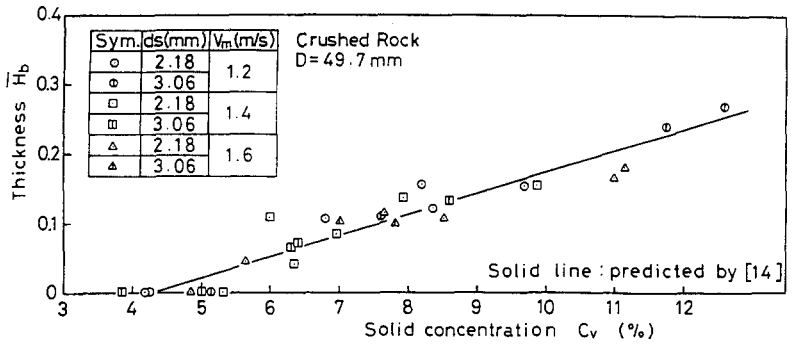

Figure 4. Effect of the solid concentration on the particle layer thickness.

3.2.3. *Height of the dunes*

Figure 5 shows the relationship between the dimensionless height of the dunes $\overline{H_{d'}}$ and the solid concentration C_v. $\overline{H_{d'}}$ is defined as follows:

$$\overline{H_{d'}} = \frac{(H_b + H)}{D} = \overline{H_b} + \overline{H}. \quad [17]$$

The value of $\overline{H_{d'}}$ increased slightly as the solid concentration increased. Some of the experimental points obtained at $V_m = 1.2$ m/s (symbols ⊙ and ⊕) showed rather large values for small concentrations. At this velocity, the flow was observed to be a stick–slip flow where the particle layer formed near the bottom wall repeatedly slid and stopped at short intervals. Thus, the flow was unstable. However, at other velocity conditions, the flow was stable or quasi-stable.

3.2.4. *Pressure fluctuation*

Figure 6 shows the maximum amplitude of the pressure fluctuation dP vs the solid concentration C_v with the particle diameter as a parameter. Tap numbers given in this figure represent the locations of the pressure transducers (refer to figure 2), and are numbered from the upstream. After Akagawa *et al.* (1970), the maximum pressure fluctuation dP was calculated from the measured probability distribution function PDI of the pressure fluctuation, according to

$$\mathrm{d}P = P(\mathrm{PDI} = 0.99) - P(\mathrm{PDI} = 0.01), \quad [18]$$

where $P(\mathrm{PDI} = 0.99)$ and $P(\mathrm{PDI} = 0.01)$ are pressures corresponding to 99 and 1% probability, respectively.

The result indicates an increasing trend of dP with the solid concentration in the range of 4–10%. However, it tends to decrease when the solid concentration exceeds 10%. This appears to be due to a change in the dune shape from triangular to flattened—i.e. when the solid concentration was $>10\%$, the shape of the dunes changed to become rather flat and the maximum amplitude of the pressure fluctuation became correspondingly smaller.

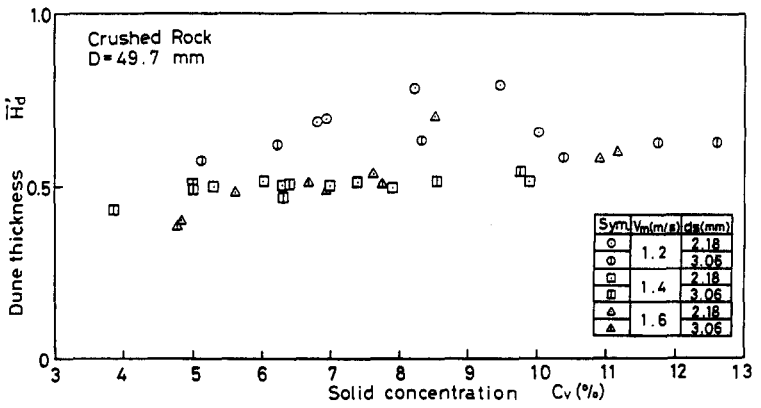

Figure 5. Effect of the solid concentration on the dune thickness.

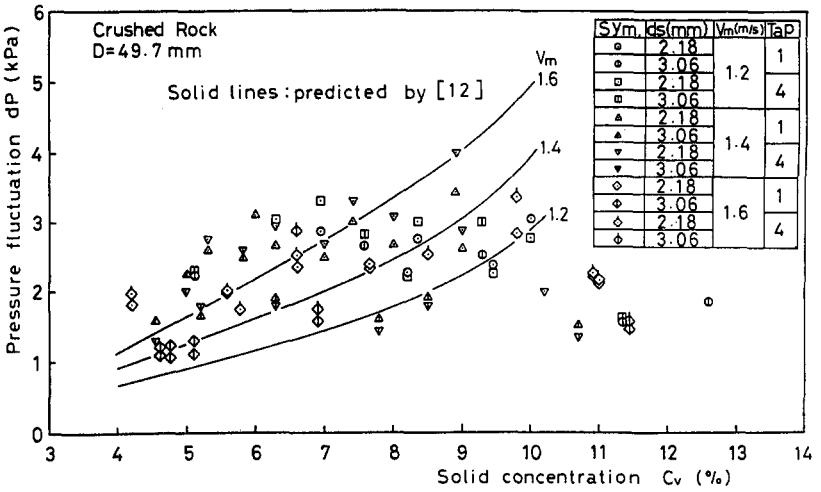

Figure 6. Relationship between the pressure fluctuation and the solid concentration.

The solid lines in figure 6 show predictions of dP by [12]. Here, ζ is 0.54 as described earlier. The porosity ϵ was determined in a still-water experiment by measuring the volume of solid particles in a measurement cell after confirming that they were settled in it. It was found that the value of ϵ was 0.55 for the two particle sizes used in this experiment. This value is not exactly the porosity in the moving particle layer. However, the porosity in the moving particle layer was assumed to be equal to that in maximum loose packing because the state of the particle layer in the pipe could be considered to be close to maximum loose packing. $\overline{A_b}$ is calculated by the following equation using [14]:

$$\overline{A_b} = \frac{(\alpha - \sin\alpha\cos\alpha)}{\pi}, \qquad \alpha = \cos^{-1}(1 - 2\overline{H_b}). \tag{19}$$

The prediction by [12] shows a general trend quite similar to that of the experiments when the solid concentration is within 4–10%. When $C_v > 10\%$, a discrepancy appears between the calculated values and the experimental ones. This is considered to be related to the change in the dune shape, as mentioned previously.

3.2.5. The PSD

In order to investigate the periodicity of the pressure fluctuation, the PSD was calculated using an FFT method. Figure 7 shows examples of the PSD of the pressure fluctuation for taps 1 and

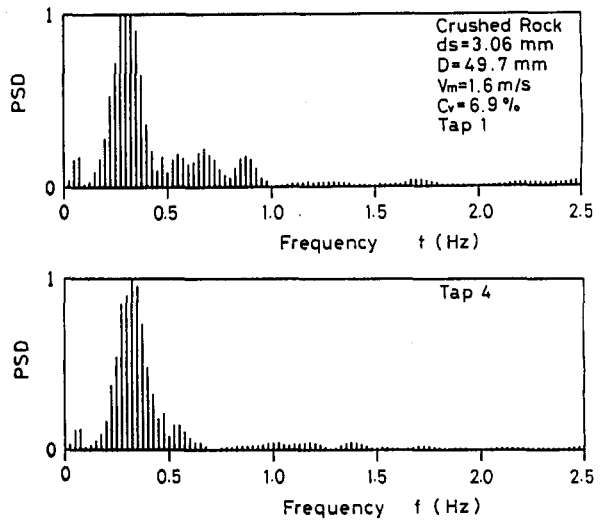

Figure 7. PSD of the pressure fluctuation.

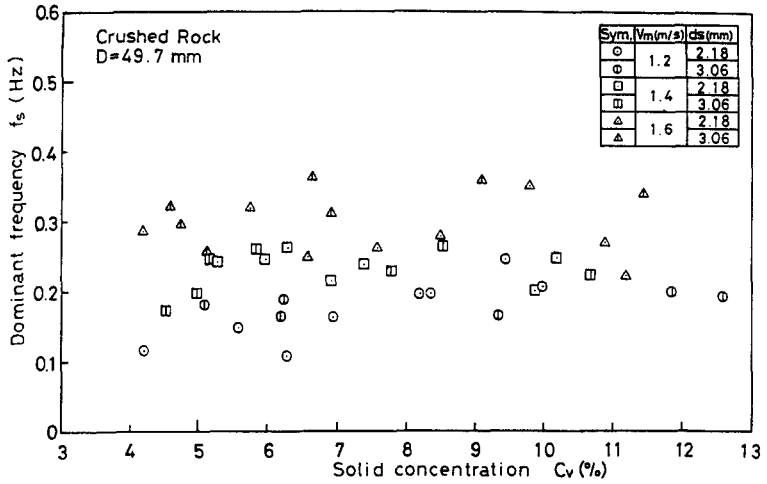

Figure 8. Relationship between the dominant frequency and the solid concentration.

4, obtained for the same experimental condition. As shown in this figure, most of the detected frequency components of the pressure fluctuation fall below 1.0 Hz. When the mean velocity was 1.6 m/s, the dominant frequency (peak frequency) was about 0.3 Hz, and hence the period was about 3 s. This conclusion leads to the simple analytical model shown in figure 1, on which the present study is based.

Figure 8 shows the dominant frequency obtained from the PSD vs the solid concentration with the mean velocity as a parameter. The data shows considerable scatter. However, it is seen that the effect of the solid concentration on the dominant frequency is negligible. On the other hand, the effect of the mean velocity is to increase the dominant frequency.

Figure 9 shows the mean dominant frequency obtained by averaging the values shown in figure 8 for each mean velocity vs mean velocity/diameter ratio (V_m/D). The mean dominant frequency is seen to be proportional to V_m/D. The solid line in figure 9 represents the following empirical equation:

$$f_s = 0.016\left(\frac{V_m}{D}\right) - 0.2, \qquad [20]$$

where f_s is the dominant frequency.

4. SIMULATION OF THE PRESSURE FLUCTUATION

There are several ways of simulating the pressure fluctuation. One of them uses the PSD. In this study, the PSD was assumed, as given by figure 10, based on the experimental observations mentioned earlier. This assumed PSD is expressed by

$$\begin{aligned} 0 < f \leqslant f_s, \quad & \mathrm{PSD}(f) = \mathrm{A}\cdot\frac{f}{f_s}, \\ f_s < f \leqslant 1, \quad & \mathrm{PSD}(f) = \mathrm{A}\frac{(1-f)}{(1-f_s)}, \\ 1 < f, \quad & \mathrm{PSD}(f) = 0, \end{aligned} \qquad [21]$$

where f is the frequency of the pressure fluctuation and f_s is the dominant frequency approximated by [20]; A is a constant.

After Hino (1977), we adopted the following calculation procedures. The pressure wave at time t, $P(t)$, is assumed to be expressed by the following equation by using its Fourier component $X(f)$:

$$P(t) = \int_{-\infty}^{\infty} X(f)\mathrm{e}^{i2\pi ft}\,\mathrm{d}f = \int_{-\infty}^{\infty} |X(f)|\,\mathrm{e}^{i(2\pi ft+\theta)}\,\mathrm{d}f, \qquad [22]$$

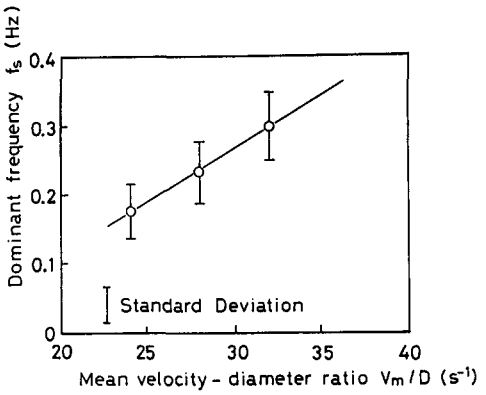

Figure 9. Relationship between f_s and V_m/D.

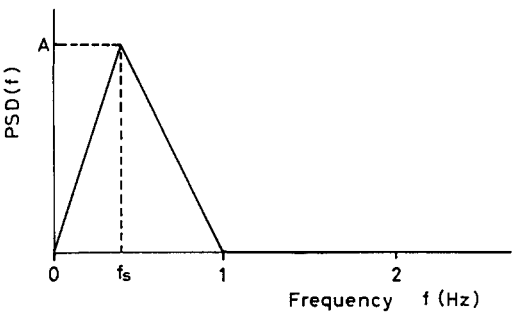

Figure 10. Assumed PSD.

where θ is a uniform random number and its range is $0 \leqslant \theta \leqslant 2\pi$. Then, the Fourier component $|X(f)|$ is expressed, using PSD(f), as

$$|X(f)| = \sqrt{T \cdot \mathrm{PSD}(f)}, \tag{23}$$

where T is the sampling time, given in terms of the sampling number N and the sampling interval Δt:

$$T = N \cdot \Delta t. \tag{24}$$

We will then define Δf_k and $\bar{f}_k$ as follows:

$$0 = f_0 < f_1 < f_2 < \cdots < f_k < \cdots < f_N = 1/2\Delta t \tag{25}$$

and

$$\Delta f_k = f_k - f_{k-1}, \quad \bar{f}_k = \frac{(f_k + f_{k-1})}{2}; \quad k = 1, 2, \ldots, N. \tag{26}$$

If [22] is approximated by the discrete components given by [25] and [26], then $P(t)$ is obtained as

$$P(t) = \sum_{k=1}^{N} \sqrt{2 \cdot \mathrm{PSD}(\bar{f}_k)\, \Delta f_k} \cos(2\pi \bar{f}_k \cdot t + \theta_k). \tag{27}$$

In this study, the sampling interval was chosen as 10 ms, as mentioned earlier, and hence $f_N = 50$ Hz. The frequency range 0–50 Hz was divided into 6144 discrete frequency segments according to [25], $P(t)$ was then calculated from [27]. These calculation procedures are described by the flow chart in figure 11.

The comparison of the simulated results with the experiments was made using the probability density function (PDF) of the pressure fluctuation. Figure 12 shows a typical result of the PDF, where P_m is the integrated average pressure. The dashed line in this figure indicates the numerical result and the solid line indicates the experimental results. As shown in this comparison, the simulated result is in good agreement with the experiments. Therefore, the assumptions used in this section i.e. figure 10 and [21], are considered to be reasonable.

5. CONCLUSIONS

A solid–liquid mixture flow at low velocities was investigated experimentally and theoretically. The following conclusions were obtained in this study:

1. The dune velocity increased as the mean velocity of the mixture increased. However, the ratio of the dune velocity to the mean velocity showed an almost constant value regardless of the solid concentration.
2. The pressure fluctuation increased slightly with the solid concentration up to 10%. On the other hand, at solid concentrations exceeding 10%, the pressure fluctuation decreased because of the change in the dune shape to flat.

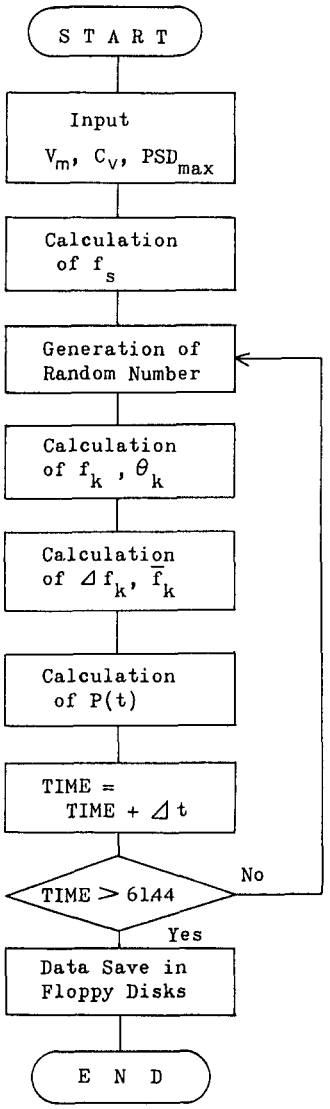

Figure 11. Flow chart of the calculation procedure.

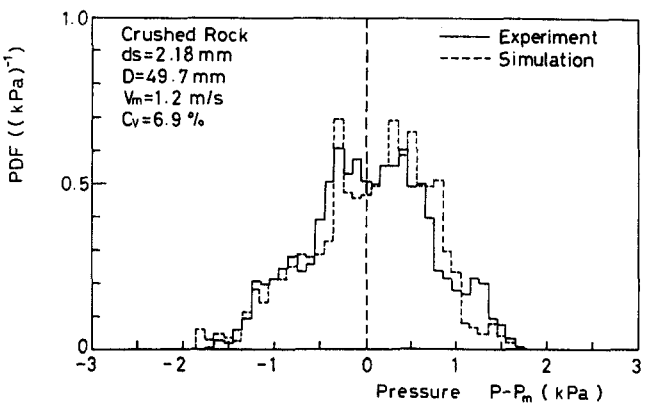

Figure 12. Comparison of the simulated results for the pressure fluctuation with the experiments.

3. It was found that the pressure fluctuation was related to the movement of dunes in the pipe. This trend is consistent with the observation that the dominant frequency in the PSD increased with an increase in the dune velocity.
4. A numerical simulation was made of the pressure fluctuation induced by a solid–liquid mixture flow at low velocities, based on a simple model. This model uses an assumed PSD of the pressure fluctuation. The results show satisfactory agreement with the experiments.

Acknowledgements—We would like to express our gratitude to Dr T. Kawashima, Emeritus Professor of Tohoku University, for his valuable discussions and also to Messrs S. Kiryu and H. Takemura for their help with the experiments.

REFERENCES

AKAGAWA, K., HAMAGUCHI, H., SAKAGUCHI, T. & IKARI, T. 1970. Study on the fluctuation of the pressure drops in two-phase flow (1st report: experimental results of the fluctuation of pressure drop in a vertical tube). *Trans. JSME* **36,** 1520–1527.

BENDAT, J. S. & PIERSOL, A. G. 1966 *Measurement and Analysis of Random Data*, pp. 200–202. Wiley, New York.

CARSTENS, M. R. 1969 A theory for heterogeneous flow of solids in pipes. *J. Hydraul. Div. ASCE* **95,** 275–286.

CONDOLIOS, E. & CHAPUS, E. E. 1963 Designing solids-handling pipelines. *Chem. Engng* **8,** 131–138.

DUCKWORTH, R. A., PULLUM, L. & LOCKYEAR, C. F. 1983 The hydraulic transport of coarse coal at high concentrations. *J. Pipelines* **3,** 251–265.

DURAND, R. 1953 Basic relationship of transportation of solids in pipes—experimental research. In *Proc. Int. Ass. of Hydraulic Research*, Minneapolis, Minn., pp. 89–103.

HINO, M. 1977 *Supekutoru Kaiseki*, pp. 142–144. Asakura Shoten, Tokyo.

KESKA, J. K. 1984 Fluctuations of the solid spatial concentration in the stationary two-phase turbulent flow of heterogeneous mixtures in pipelines. *J. Pipelines* **4,** 149–157.

MISCOE, A. J. & FADDICK, R. R. 1980 U.S. Department of energy hydraulic transport research facility for coarse coal. In *Proc. 5th Int. Conf. on Slurry Transportation*, pp. 136–143.

NEWITT, D. M., RICHARDSON, J. F., ABBOTT, M. & TURTLE, R. B. 1955 Hydraulic conveying of solids in horizontal pipes. *Trans. Instn chem. Engrs* **33,** 93–113.

NODA, K., MASUYAMA, T. KAWASHIMA, T. & HASHIMOTO, H. 1980 Influence of pipe inclination on deposit velocity. In *Proc. 7th Int. Conf. on the Hydraulic Transport of Solids in Pipes*, BHRA, Cranfield, U.K., Paper F2.

NODA, K., TAKAHASHI, H. & KAWASHIMA, T. 1984 Relation between behavior of particles and pressure loss in horizontal pipes. In *Proc. 9th Int. Conf. on the Hydraulic Transport of Solids in Pipes*, BHRA, Cranfield, U.K., Paper D4.

SHOOK, C. A. & DANIEL, S. M. 1965 Flow of suspensions of solids in pipelines: Part I. Flow with a stationary deposit. *Can. J. chem. Engng* **43,** 56–61.

SHOOK, C. A., HASS, D. B., HUSBAND, W. H. W., SMALL, M. & GILLIES, R. 1981 Pipeline flow of coarse coal slurries. *J. Pipelines* **1,** 83–92.

TELEVANTOS, Y., SHOOK, C. A., CARLETON, A. & STREAT, M. 1979 Flow of slurries of coarse particles at high solids concentrations. *Can. J. chem. Engng* **57,** 255–262.

TODA, M., YONEHARA, J., KIMURA, T. & MAEDA, S. 1977 Transition velocities in horizontal solid–liquid two-phase flow. *Kagaku Kogaku Ronbunshu* **3,** 497–503.

TODA, M., YONEHARA, J. & MAEDA, S. 1978 Horizontal solid–liquid two-phase flow at low flow rates. *Kagaku Kogaku Ronbunshu* **4,** 361–365.

TODA, M., KONNO, H. & SAITO, S. 1980 Simulation of limit deposit velocity in horizontal liquid–solid flow. In *Proc. 7th Int. Conf. on the Hydraulic Transport of Solids in Pipes*, BHRA, Cranfield, U.K., Paper J2.

TSUJI, M., MORIKAWA, Y., SUGIMOTO, S., MIYOSHI, S. & NAKANO, Y. 1982 Flow pattern and pressure fluctuation in air–solids two-phase flow in a pipe at low velocities. *Trans. JSME* **48,** 656–663.

TSUJI, Y., MIYOSHI, S. & MORIKAWA, Y. 1984 Kokinisoryu no fuanteiryudo. In *Proc. 3rd Multiphase Flow Symp.*, Tokyo, Japan, pp. 97–110 (in Japanese).

WILSON, K. C., STREAT, M. & BANTIN, R. A. 1972 Slip-model correlation of dense two-phase flow. In *Proc. 2nd Int. Conf. on the Hydraulic Transport of Solids in Pipes*, BHRA, Cranfield, U.K., Paper B1.